

# Research on Movement Monitoring and Law of Overlying Strata in Goaf Based on IMU Technology

<sup>1st</sup> Shiliang Wu <sup>1,2</sup>, <sup>2nd</sup> Zhengwen Chen<sup>1,2</sup>, <sup>3rd</sup> Zheng Xue <sup>1,2</sup>

<sup>1</sup>College of Energy and Mining Engineering, Shandong University of Science and Technology, Qingdao China 266590.

<sup>2</sup>Shandong University of Science and Technology Mine Disaster Prevention and Control Provincial and Ministry Co-construction National Key Laboratory Cultivation Base, Qingdao China 266590.

**Abstract**—The overlying strata of the stope can be divided into low ( immediate roof ), medium and high strata according to the degree of influence of the mine pressure behavior of the working face. Among them, the pressure step distance of low rock strata can be judged according to the roof pressure appearance of hydraulic support, and the middle and high rock strata can not be accurately and intuitively determined only by theoretical calculation. Therefore, IMU is used to monitor the motion state and fracture distance of different layers, so as to study the relationship between them and periodic weighting. Firstly, the accuracy of monitoring effect and the error of monitoring data are determined by indoor test. Then, taking the 52507 working face of Daliuta as the engineering background, 3DEC software is used to assist the verification. The research shows that the IMU monitoring data meets the requirements of error and accuracy, and can accurately monitor the rock movement ; the movement period of rock strata at different heights is different. As the height of rock strata increases, the displacement distance of rock strata gradually increases, and the median rock strata play a key role in the movement of overlying rock strata. The periodic pressure monitored is twice the actual periodic pressure.

## 1 Introduction

With the advancement of the working face, the mining area is increasing, and the mine pressure of the overlying strata in the goaf is gradually obvious, which is easy to produce strong mine pressure, which is not conducive to the safe mining of the working face<sup>[1-4]</sup>. Therefore, it is very important to monitor the movement of overlying strata in goaf. At present, the effective monitoring methods of rock strata movement in China are different. In the past, the movement law of roof strata was determined by theoretical calculation combined with observation and analysis of mine pressure in working face, and the development height of ' two zones ' was determined by drilling technology and engineering analogy method, but they all have certain limitations<sup>[5-7]</sup>. The theoretical calculation and observation content can not meet the actual complex and changeable geological conditions and strata movement<sup>[7-12]</sup>.

Secondly, Tan Yunliang<sup>[13]</sup> et al. predicted the roof caving by using the roof deflection deformation value, and the prediction threshold has a large difference with the roof lithology. The emergence of the peak section of the roof separation velocity is used as a method to predict the lower roof caving. Liang Yunpei<sup>[14]</sup> through the roof fracture generated by the small vibration, through the microseismic system to analyze the roof movement. These are through the external mine pressure

characteristics to infer the law of overlying strata movement, no direct observation of the roof movement state.

Nowadays, IMU technology has matured, which can accurately capture small changes in displacement and angle in real time, and can rely on communication modules for data transmission to achieve real-time ground monitoring<sup>[15-20]</sup>. Now Shandong mining Daliuta coal mine 52507 working face initial weighting step distance of 40-70 m, suspended roof area is large, difficult to collapse. In order to reduce the caving step distance, the roof hydraulic fracturing treatment was carried out in Shandong mining area. The roof will break in a small area, resulting in the change of displacement and angle of rock strata. In this paper, IMU monitoring method is used to directly monitor the motion state of rock strata and realize accurate real-time monitoring.

## 2 Basic Principle of IMU Monitoring System

With the working face mining, the overlying strata will produce relative movement under the influence of stress changes, which is usually accompanied by changes in displacement and angle. Therefore, multiple sets of IMU monitoring units can be used to collect parameters such as displacement and angle of overburden movement, and the data is transmitted to the host computer system and displayed in a three-dimensional map by computer.

\* Corresponding author: 569069738@qq.com

The three core parameters of euler angle are roll angle  $\gamma$ , heading angle  $\varphi$  and pitch angle  $\theta$ . The corresponding matrix in the coordinate system is:

Y axis - heading angle  $\varphi$ ,

$$A_1 = \begin{bmatrix} \sin \varphi & -\sin \varphi & 0 \\ \sin \varphi & \cos \varphi & 0 \\ 0 & 0 & 1 \end{bmatrix} \quad (1)$$

Z axis - pitch angle  $\theta$ ,

$$A_2 = \begin{bmatrix} 1 & 0 & 0 \\ 0 & \cos \theta & \sin \theta \\ 0 & -\sin \theta & \cos \theta \end{bmatrix} \quad (2)$$

X axis - roll angle  $\gamma$ ,

$$A_3 = \begin{bmatrix} \cos \gamma & 0 & -\sin \gamma \\ 0 & 1 & 0 \\ \sin \gamma & 0 & \cos \gamma \end{bmatrix} \quad (3)$$

The change matrix of geographic coordinate system (n system) and carrier coordinate system (b system) is:

$$A_n^b = (A_n^b)^T = A_3 A_2 A_1 = \begin{bmatrix} \cos \gamma \cos \theta + \sin \gamma \sin \theta & -\sin \gamma \cos \varphi + \sin \gamma \sin \theta \cos \varphi & -\sin \gamma \cos \theta \\ \cos \theta \sin \varphi & \cos \theta \cos \varphi & \sin \theta \\ \sin \gamma \cos \varphi - \cos \gamma \sin \theta \sin \varphi & -\sin \gamma \cos \varphi - \sin \gamma \sin \theta \cos \varphi & \cos \theta \cos \gamma \end{bmatrix} \quad (4)$$

The relationship between the angular velocity matrix of system b relative to system n and the vector  $\dot{\theta}$ ,  $\dot{\gamma}$ ,  $\dot{\varphi}$  is :

$$\omega_{nb}^b = [\omega_z \ \omega_\gamma \ \omega_\varphi]^T \quad (5)$$

After arrangement:

$$\begin{cases} \dot{\gamma} = \sin \gamma \tan \theta \omega_z + \omega_\gamma - \cos \gamma \tan \theta \omega_\varphi \\ \dot{\theta} = \omega_z \cos \gamma + \omega_\gamma \sin \gamma \\ \dot{\varphi} = (\omega_z \sin \gamma - \omega_\gamma \cos \gamma) \sec \theta \end{cases} \quad (6)$$

### 3 Data acquisition and error analysis

The data acquisition range mainly includes the acquisition of the vertical displacement of the carrier moving downward and the real-time angle of the carrier attitude angle. Therefore, the test content is mainly divided into two parts: vertical displacement test and error analysis, attitude angle rotation test and error analysis are shown in Table 1.

TABLE 1 VERTICAL DISPLACEMENT AND ATTITUDE ROTATION ANGLE ERROR ANALYSIS

Vertical ground height	Vertical displacement/mm				Attitude angular/°		
	Monitoring 1	Monitoring 2	Monitoring 3	Average error	Actual angle	Acquisition angle	Error
100	80	79	91	16.66	0	1.1	1.1
150	130	120	144	18.66	10	8.7	1.3
200	186	178	176	20	20	18.9	1.1
600	550	540	566	48	30	29.3	0.7
800	755	761	775	36.33	40	38.1	1.9
1000	973	956	968	35.33	50	48.7	1.3

According to the test results, when  $h = 100, 150, 200, 600, 800, 1000$ mm, the average error of vertical displacement and attitude angle is 16.66, 1.1 ; 18.66, 1.3 ; 20, 1.1 ; 48, 0.7 ; 36.33, 1.9 ; 35.33, 1.3. In summary, when the sensor is doing downward free fall motion, the error of vertical displacement basically meets  $< 10\%$ , and the angle error of attitude angle basically meets  $< 2^\circ$ . The sensor can collect values normally and meet the accuracy requirements.

### 4 Experimental verification of roof caving

The experimental design model parameters are as follows : 50m above the coal seam roof strata are mainly sandy mudstone ( 1.82m ) ; fine-grained sandstone ( thickness 8.16 m ) ; siltstone ( thickness 18.09 m ). It is assumed that the siltstone with a thickness of 18.09 m is the basic top ( key layer ), and its initial weighting interval is 60 m and the periodic weighting interval is 16 m. In order to better simulate the roof displacement and caving effect, the mining height of some models is increased to 2 ~ 3

times of the original mining height. The geometric similarity ratio refers to the spatial similarity ratio between the model and the prototype. In this experiment, the basic roof fracture step distance of 60 ~ 80 m is equivalent to the model of 600 ~ 800 mm as the similarity ratio.

$$a_m = \frac{L_p}{L_m} = 100 \quad (7)$$

Where:  $a_m$ -model similarity ratio;  $L_p$ - prototype step length;  $L_m$ - model step length.

Model stacking effect is shown in the figure, the sensor is placed in the rock, so that the rock movement can be accurately monitored. A total of five measuring points are set up, which are the locations of each data acquisition sensor, as shown in Figure 1.

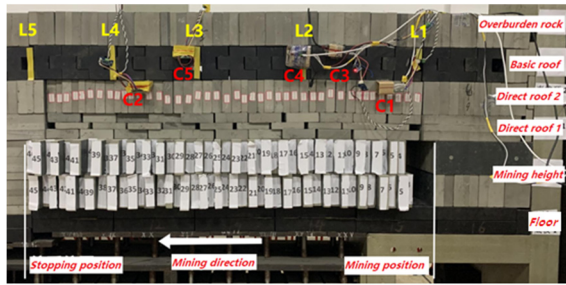


**Figure 1.** Monitoring sensor location diagram

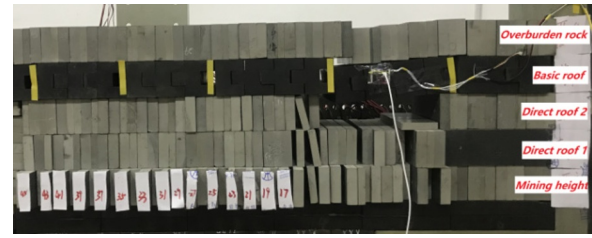
L1 ~ L3 is the first weighting step, L3 ~ L4 is the first periodic weighting step, L4 ~ L5 is the first periodic weighting step. L1 is the edge fracture line of the first weighting step, which is 60 mm relative to the mining position of the working face; L2 is the central fracture line of the first weighting step, relative to the working face mining position 420 mm; L3 is the first periodic weighting step fracture line, relative to the working face mining position 780mm; L4 is the central fracture line of the second periodic weighting step, relative to the working face mining position 1050 mm; L5 is the second periodic weighting step edge fracture line, relative to the working face mining position 1290mm.

The two measuring points of the immediate roof are C1 ~ C2 from right to left: C1 is 210mm from the mining position, and C2 is 930mm from the mining position. C1 ~ C2 can collect the roll angle displacement and collapse displacement of the measuring point.

The three measuring points of the main roof, from right to left, are C3 ~ C5: C3 is 330mm from the mining position, C4 is 420mm from the mining position, and C5 is 780mm from the mining position. C3 ~ C5 can collect the pitch angle displacement and collapse displacement.

Mining every draw a 30mm wide plate block as a knife, that is, mining pace, a total of 46 knife. Plate blocks are digitally marked from 1 to 46.

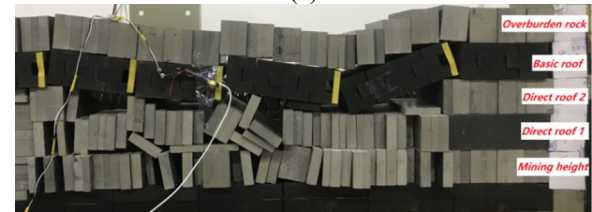
Roof movement is shown in Figure 2.



(a)



(b)



(c)

**Figure 2.** Test roof movement

The first layer of immediate roof will collapse with mining, and the second layer of immediate roof is affected by the first layer of immediate roof to produce structural collapse. When the working face advances to the third knife 90mm, the first layer of immediate roof falls for the first time, and the second layer of immediate roof produces a slight flip angle displacement. When advancing to 5 knife 150mm, the second layer of immediate roof collapses for the first time, after each advance of about 2 ~ 3 knife 60 ~ 90m will produce a immediate roof collapse, when advancing to 46 knife 1380mm, two layers of immediate roof collapse completely.

Motion characteristics and parameters of model main roof are shown in Table 2.

**TABLE 2** MOTION CHARACTERISTICS AND PARAMETERS OF MAIN ROOF OF MODE

Progress / knife	Progress /mm	Basic Roof Position Description	Basic Top State Description	Actually Measured Parameters
12	360	Within initial pressure step L1	Fracture at L1, but no obvious displacement	-
14	420	Within initial pressure step L1~L2	Fracture at L2, and produce significant subsidence displacement, L1 ~ L2 form a suspended state	L1~L2 overhang angle: 8°
20	600	Within initial pressure step L1~L2	L2 caving touch gangue, L1~L2 still suspended state	L1~L2 overhang angle: 15°
25	750	Within initial pressure step L2~L3	Fracture at L3, L2~L3 form a suspended state	L2~L3 overhang angle: 12°
37	1110	Within initial pressure step L2~L3、The first cycle pressure step distance L3~L4	L2~L3 completely collapse contact gangue, L4 fracture, L3~L4 form hanging state	L2~L3 contact angle: 5° L3~L4 overhang angle: 24°
46	1380	The first cycle pressure step distance L3~L4、The second cycle pressure step distance L4~L5	L3~L4 completely collapse contact gangue, L5 fracture, L4~L5 form hanging state	L3~L4 contact angle: 3° L4~L5 overhang angle: 10°

It can be seen from the above figures and tables that:

(1) The movement parameters and states of immediate roof and main roof in the process of model mining are systematically tested by using data acquisition sensors, and the parameters of roof movement under specific mining conditions are obtained, including : the rotation angle and caving displacement of immediate roof, the rotation angle and caving displacement of main roof.

(2) When the angle of the immediate roof measuring point changes but no collapse displacement data is generated, it is judged that the rock block where the measuring point is located is in an inclined state and no caving occurs. If the collapse displacement data is generated, it is judged that the caving has occurred. If the angle change of the backward rock mass occurs again, it is judged that the second rolling occurs, otherwise it is judged that it is stable.

(3) When the angle of the measuring point of the main roof changes but no collapse displacement data is generated, it is judged that the rock mass in the section where the measuring point is located is in the suspended state and the measuring point is not collapsed. If the collapse displacement data is generated or the rock mass in the section is in the quasi-horizontal state, it is judged that it is completely collapsed ( due to the influence of the measurement accuracy of the instrument, the smaller mining height of the model 1 leads to the smaller collapse displacement space of the main roof, so it can only be judged that the rock mass in the section where the measuring point is located is in the suspended state and can not accurately judge whether the measuring point is collapsed. However, when the angle of rock mass changes from inclined overhanging state to horizontal or quasi-horizontal state, it can be judged that it has completely collapsed. If the angle change occurs again after the collapse of the rock mass, it is judged that the second rolling occurs, otherwise it is judged that it is stable.

(4) the sensor after multiple model mining value, stable operation, accurate data acquisition.

## 5 Site monitoring point arrangement

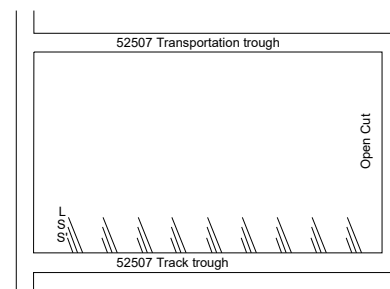
The 52507 fully mechanized mining face of Daliuta Coal Mine is located in the fifth panel of No.52 coal seam in Daliuta well. The buried depth is 88.63-189.37 m, the length of the working face is 3871.80 m, the width of the working face is 301.0, the area is 1.1654 million m<sup>2</sup>, the dip angle of the coal seam is 1-3 °, the thickness of the coal seam is 6.8-7.62 m, and the average is 7.3 m. It belongs to the stable coal seam. The rock column diagram of Daliuta coal mine is shown in Table 3.

TABLE 3 DALIUTA COAL MINE STRATA HISTOGRAM

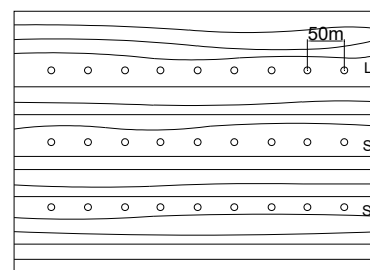
Level Number	Rock Name	Thickness of Stratum/m	Roof Height/m
1	drift sand	5	175.5
...	...	...	...
24	medium grained sandstone	1.6	88.9
25	sandstone	4.9	87.3
26	medium grained sandstone	3.2	97.1

...	...	...	...
34	coal	1.1	69.3
35	sandstone	10.8	68.2
36	fine-sandstone	2.5	57.4
...	...	...	...
51	fine-sandstone	5.4	31.2
52	medium grained sandstone	5.7	25.8
53	sandstone	0.8	20.1
54	coarse sandstone	19.3	19.3
55	5-2 coal	7.65	0
56	carbon mudstone	1.95	-1.95

Through the key layer theory [4], the low, medium and high rock strata are located and judged. Through the arrangement of rock strata at different positions, the first drilling arrangement is located at 40 m of the cutting hole, as shown in Figure 3.



(a)plane diagram



(b)section diagram

Figure 3. IMU monitoring device layout diagram

Drilling parameters of IMU monitoring device are shown in Table 4.

TABLE 4 DRILLING PARAMETERS OF IMU MONITORING DEVICE

Drilling Type	Height /m	Horizontal Distance /m	Arrangement Spacing /m	Dip angle /°	Direction	Number
L	54	35	200	47	Vertical coal wall	10
S	40	34	100	50	Vertical coal wall	10
S'	17	15	50	41	Vertical coal wall	10

There are 1 measuring point in L, S, S' borehole at the cutting hole, a total of 3 measuring points, and 9, 9, 9 measuring points in 52507 Huishun L, S, S' borehole, a total of 30 measuring points.

## 6 Overall analysis of rock displacement

According to the analysis of the observation results after the advance of the working face, 300m before the advance of the working face is selected, the daily average advance is relatively uniform, and the coal seam is excessively gentle, which can clearly show the advance process of the whole working face. The change of roof displacement is shown in Figure 4.

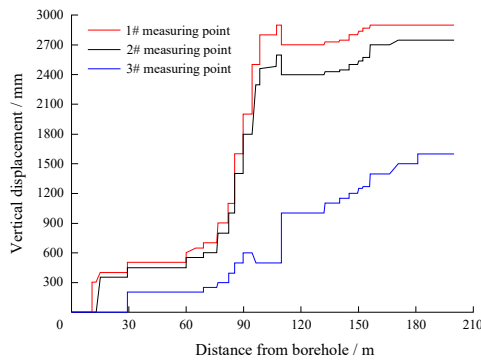


**Figure 4.** The first group of borehole rock displacement change diagram

From the trend shown in Figure. 4, the following characteristics of strata movement can be summarized:

(1) After the rock stratum exceeds the maximum bearing force, the displacement appears 'step', and finally the fluctuation range becomes smaller to a relatively stable equilibrium state.

(2) With the advance of the working face, the low rock strata monitored by 1 # measuring point has a vertical abrupt displacement of about 300mm at 10m behind the borehole, which indicates that the low rock strata have fractured and deformed here. With the advance of the working face, the medium rock layer monitored by the 2 # measuring point has a vertical mutation displacement of about 350 mm at a lag of 15.1 m behind the borehole, indicating that the medium rock layer has broken and deformed here. The vertical displacement of the low rock stratum is 94mm under the influence of the fracture deformation of the middle rock stratum, and the rotation at 110m also follows this law. When the working face is pushed to 110 m behind the borehole, the low strata and the middle strata tend to be stable, indicating that the full subsidence deformation occurs and tends to be relatively stable.

(3) The same influence principle, when the 3 # measuring point monitoring of high rock strata with the advance of the working face lags behind the borehole 29.2m occurred about 200mm vertical displacement mutation, but at this time by the influence of high rock strata movement, the middle rock strata and low rock strata were 54mm, 50mm mutation; at 110 m, affected by the rotation of the median rock stratum, the high rock stratum suddenly sank by about 400 m.

(4) It can be roughly seen that the initial breaking step distance of the low rock stratum is 50.8m, the breaking step distance of the middle rock stratum is 58m, and the breaking step distance of the high rock stratum is 70.1m.

(5) The frequency of breaking: low rock > medium rock > high rock, and the medium rock plays a connecting role in the key strata of the roof.

## 7 Analysis of Relationship between Fracture Frequency and Periodic Pressure

According to the analysis in the previous section, it can be seen that in the rock movement monitored by IMU, the frequency of fracture in low rock strata is the largest, and the frequency of fracture decreases with the deepening of rock height. We selected the data of three groups of measuring points to compare and analyze the relationship between the fracture frequency and the periodic pressure. As shown in Figure 5.

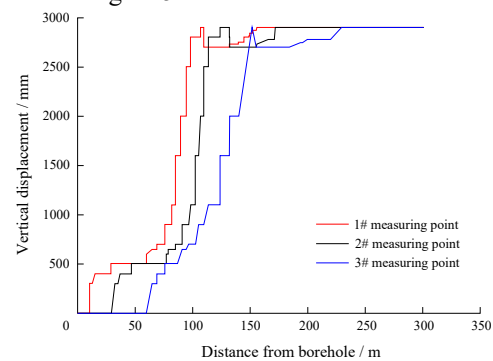


**Figure 5.** Displacement diagram of three monitoring boreholes

It can be seen from Fig.4 that the step distances of three periodic weighting in 52507 working face are 26 m, 28.5 m and 31 m respectively, and the average weighting period is 28.5 m. In order to further verify the accuracy of the pressure cycle, we selected Daliuta coal mine 52507 working face support working resistance data shown in Table 5

**TABLE 5** PERIOD PRESSURE DATA STATISTICS TABLE

Date	Distance from Open-off Cut /m	Periodic Weighting Step /m
3.1	30	17.9
3.3	45	12
3.5	56	14.5
3.7	67	9.6
3.9	85	15.2
3.11	95	10
3.13	110	13.9
3.15	129	17.1
3.17	142	11.4
3.19	156.2	11.2
3.21	165.6	15.4
3.23	177	10.4
3.25	191	14.7
3.27	210	16.1
3.29	236	14.1
3.31	250	14.7

Calculated from Table 5, the average weighting period in March is about 14.06 m. By comparing the line chart of Fig.5, it can be clearly analyzed that the average period of displacement of the two monitoring boreholes is 28.5 m, which is about 2 times the actual pressure period. The results show that it is scientific to study the law of overlying strata by using IMU monitoring borehole



displacement cycle as the basis for judging rock movement.

## 8 Numerical Simulation Verification

In order to reflect the law of rock overburden movement during the mining of 52507 working face, according to the comprehensive histogram of coal seam roof and floor, considering the factors such as overburden rock properties and boundary conditions in the field mining range, the final design model X \* Y \* Z is 400m \* 5m \* 200m, and The mechanical parameters are shown in Table 6.

the mining thickness of coal seam is 7.5m. Create a numerical model as shown in Figure 6.

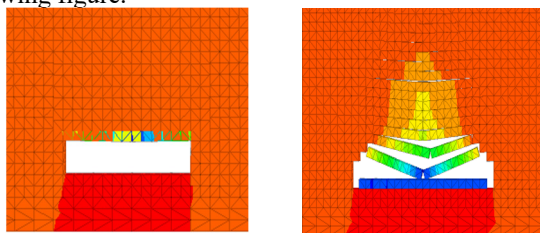


Figure 6. 3DEC numerical simulation model

TABLE 6 PARAMETERS OF ROCK MECHANICAL PROPERTIES

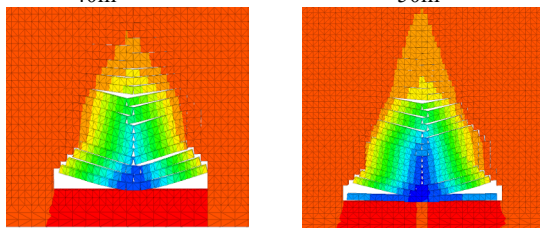
Rock Stratum Name	Density/Kg·m <sup>-3</sup>	Elastic Modulus/GPa	Poisson Ratio	Force of Cohesion/MPa	Angle of Internal Friction/°
mudstone	2100	12	0.19	4.8	27
sandstone	2340	11	0.2	5.1	27
fine-sandstone	2230	8.6	0.2	4.56	22
Medium-grained sandstone	2420	10	0.23	3.78	24
Coarse grained sandstone	2380	18	0.22	4	23
Rock siltstone	2400	8.8	0.21	3.5	25
5-2 coal	1400	10	0.2	1.14	20

The working face excavation process is shown in the following figure.



(a) Working face advancing 40m

(b) Working face advancing 50m



(c) Working face advancing 60m

(d) Working face advancing 70m

Figure 7. Working face advancing overburden movement simulation diagram

According to Figure 7, the following conclusions can be drawn :

When the working face advances 40m, the roof appears cracks, but does not collapse.

When the working face advances 50 m, the immediate roof begins to collapse, accompanied by displacement changes.

When the working face advances 60 m, the median rock stratum breaks, which affects the low rock stratum and increases the displacement of the immediate roof.

When the working face advances 70 m, the high-position rock stratum breaks, which in turn affects the low-position rock stratum and the middle-position rock

stratum, increasing the vertical displacement of the two layers.

Through the above numerical simulation and monitoring data, it can be obtained that the initial caving step distance of low rock is about 50m, the initial caving step distance of medium rock is about 60m, and the initial caving step distance of high rock is about 70m.

## 9 Conclusion

(1) When the sensor does downward free fall motion, the error of vertical displacement basically meets < 10 %, and the angle error of attitude angle basically meets < 2 °. The sensor can collect values normally and meet the accuracy requirements.

(2) Through IMU monitoring, the vertical displacements of low, medium and high rock strata are obtained, and they can influence each other. The first fracture cycle is 50m, 58m, 70m ; the size of the displacement rises in turn.

(3) By comparing the four groups of monitoring data of low rock strata, it can be obtained that the pressure period is 28.5m, and the pressure period presented by the working resistance of the support is 14.06m. The pressure period presented by the monitoring data is about twice that of the support data, which verifies the reliability of IMU monitoring.

(4) Using 3DEC to verify the distribution law of the first caving cycle of different rock strata, it is basically consistent with the monitored data, which proves that the IMU monitoring system can accurately monitor the movement law of rock strata.

## REFERENCES

1. Gao Zeming. Study on the development height of water-conducting fractures in overlying strata of goaf [J].Coal technology, 2021,40 (01) : 78-81.DOI : 10.13301 / j.cnki.ct.2021.01.02.
2. Xu Guosheng, Xu Shengjun, Li Dehai and so on. Simulation analysis of stress recovery law of overlying strata in goaf [J].Coal technology, 2021,40 (08) : 8-11.DOI : 10.13301 / j.cnki.ct.2021.08.003.
3. Yan Fei. Analysis and measurement of ' three zones ' height of overlying strata in goaf [J].Coal technology, 2021,40 (11) : 54-56.DOI : 10.13301 / j.cnki.ct.2021.11.012.
4. Zhang Peipeng, Jiang Lishuai, Liu Xufeng and so on. The evolution characteristics and disaster-causing law of mining overburden structure in high hard and thick strata [J]. Journal of Mining and Safety Engineering,2017,34(05):852-860.DOI:10.13545/j.cnki.jmse.2017.05.005.
5. Wu Shiliang, Meng Baowei, Han Wei.A method based on 6-axis inertial measurement unit to monitor mining overburden movement : CN202011099916.9 [P] 2021-02-09.
6. Chen Xiaozhen, Zhou Jiao, Dong Yanqin, et al. Application of big data theory in high-precision inertial navigation system test technology [J]. Navigation and control,2018,17(1):11-20,33. DOI: 10.3969 / j.issn.1674-5558.2018.01.002.
7. Chen Weina, Yang Zhong, Tang Yujuan and so on. Research on information fusion method of adaptive inertial / land-based integrated navigation system [J].Journal of Jinling Institute of Technology, 2022,38 (03) : 48-55.DOI : 10.16515 / j.cnki.32-1722 / n.2022.03.007.
8. Wang Wanjie, Gao Fuqiang. Study on physical and numerical simulation of mining-induced fracture evolution law of overlying strata in working face [J/OL].Journal of Mining and Strata Control Engineering : 1-10 [2023-04-06].<https://doi.org/10.13532/j.jmsce.cn10-1638/td.20230308.001>.
9. Jia Dong, Jiang Deyi, Chen Jie et al. Similar simulation test on failure characteristics and fracture evolution of overlying strata in fully mechanized caving face [J/OL].China Safety Production Science and Technology,2022(03):1-7[2023-04-06].<http://kns.cnki.net/kcms/detail/11.5335.TB.20220127.0906.002.html>.
10. Ma Fuwu, Li Yang, Su Huairui, et al. Analysis of fracture evolution characteristics and disaster mechanism of overlying rock under hard and thick strata [J].Coal Engineering, 2023,55 (2) : 93-97. DOI : 10.11799 / ce202302017.
11. Zhang Guojun. Study on mine pressure law of overlying strata in extremely shallow coal seam group [J].Coal technology, 2022,41 (10) : 24-28.DOI : 10.13301 / j.cnki.ct.2022.10.006.
12. Zhao Yixin, Ling Chunwei, Liu Bin, etc. Study on fracture evolution and energy dissipation law of overlying strata in shallow buried super-large mining height working face [J].Journal of Mining and Safety Engineering, 2021,38 (01) : 9-18 + 30.
13. Xu Jialin, Qian Minggao.Discrimination method of key strata position of overlying strata [J].Journal of China University of Mining and Technology, 2000,29 (5) : 463-467. DOI : 10.3321 / j.issn : 1000-1964.2000.05.005.
14. Tan Yunliang, He Kongxiang, Ma Zhisheng, et al..Research on separation layer telemetry prediction system of hard roof caving [J].Journal of Rock Mechanics and Engineering, 2006,25 (8) : 1705-1709.
15. Yun Liang Yunpei, Wang Haibin, Li Quanguai, et al. Study on the movement law of overlying strata in nearly horizontal thick coal seam based on microseismic monitoring [J].Mining safety and environmental protection,2021,48(6):6-11,18.DOI:10.19835/j.issn.1008-4495.2021.06.002.
16. Gong Yilin. Research and implementation of adaptive integrated navigation system based on IMU aided update detection [D]. Beijing University of Posts and Telecommunications, 2021.DOI : 10.26969 / d.cnki.gbydu.2021.001300.
17. Cui Xiaozhen, Zhou Qi, Wu Dongjie et al. GNSS / IMU and odometer tightly-loosely coupled factor map fusion positioning method [J/ OL].Journal of Wuhan University ( Information Science Edition ) : 1-15 [2023-04-06].<http://kns.cnki.net/kcms/detail/42.1676.TN.20230403.1832.006.html>.
18. Wang Jingxiao, Liu Ning, Su Zhong et al. Design of MEMS-IMU automatic calibration system for high-spin projectile [J/OL]. Electro-optic and control:1-7[2023-04-06]. <http://kns.cnki.net/kcms/ detail/41.1227.TN.20230322.1657.002.html>.
19. Hu Wenlong, Zhou Yufei, Song Quanjun, et al. Research on indoor positioning algorithm based on UWB and IMU information fusion [J]. Manufacturing automation, 2023,45 ( 2 ) : 193-197,213. DOI : 10.3969 / j.issn.1009-0134.2023.02.039.
20. Xu Aigong, Du Jian, Sui Xin and so on. The application of zero-velocity correction and complete monitoring in UWB / MEMS IMU combination [J]. Surveying and Mapping Science, 2022,47 (12) : 1-7 + 65.DOI : 10.16251 / j.cnki.1009-2307.2022.12.001.